Structure *19*

Supplemental Information

Structural Basis for Complex Formation between Human IRSp53 and the Translocated Intimin Receptor Tir of Enterohemorrhagic *E. coli*

Jens C. de Groot, Kai Schlüter, Yvonne Carius, Claudia Quedenau, Didier Vingadassalom, Jan Faix, Stefanie M. Weiss, Joachim Reichelt, Christine Standfuß-Gabisch, Cammie F. Lesser, John M. Leong, Dirk W. Heinz, Konrad Büssow, and Theresia E.B. Stradal

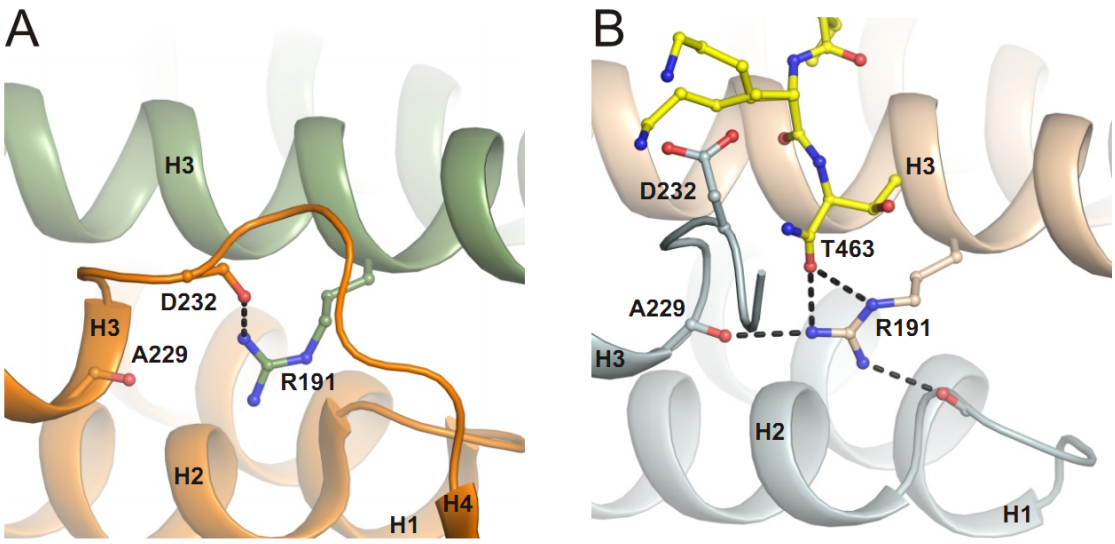

Figure S1, related to Figure 3: Comparison of helix H4 in free I-BAR$_{IRSp53}$ and in the peptide complex. (A) In the free structure (PDB 1Y2O), Arg191 of one monomer (green) binds to the loop linking helix H3 and helix H4 of the other monomer (orange) and thereby stabilizes helix H4 adjacent to the dimer. In the structure of the complex (B), the peptide's terminal amide group (yellow) binds to the guanidinium group of Arg191 of one I-BAR monomer (wheat), leading to a conformational change of helix H4 and the preceding loop of the other monomer (blue).

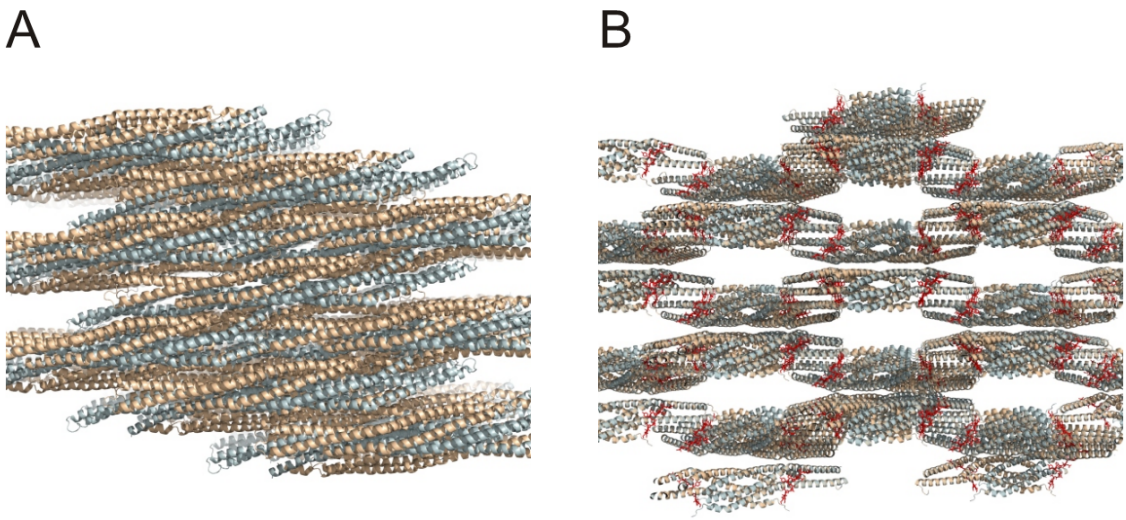

Figure S2, related to Figure 1: Different crystal packing of free versus peptide loaded I-BAR domain of IRSp53. While the individual fold of each I-BAR is highly similar, crystal packing of free versus peptide bound I-BARs significantly differs. (A) Crystal packing according to Millard *et al.* of the free I-BAR (PDB entry 1Y2O). I-BARs are densely packed. The two protomers of each dimer are in cyan and wheat, respectively. (B) Crystal packing of the peptide loaded I-BAR displays a more loose array, explaining the undetectability of the loop between H2 and H3 and of entire H4. Tir peptides are shown in red.

Table S1: primers used in this study

Primers	**5' Sequence 3'**
pGEX fwd (I-BAR)	GGGCTGGCAAGCCACGTTTGGTG
I-BAR rev	GACTGCGGCCGCTCAGTTGCTGGCCACCTGC
L28E fwd	CTAGCgaaCGGAACTTCATaGCCATGGG
L28E rev	GTTCCGttcGCTAGGGTTGAAtTGCTCCATG
K108 fwd	GCAGCTGGAGCAGgcGGTGGAGCTGGACT
K108 rev	AGTCCAGCTCCACCGCCTGCTCCAGCTGC
R193S fwd	GAGCGCAGGaGCTTCTGCTTCtTGGTGGAGAAG
R193S rev	CTTCTCCACCAGGAAGCAGAAGCTCCTGCGCTC
F196A fwd	GAGCGCAGGCGCTTCTGtgcaCTGGTGGAGAAG
F196A rev	GAGCGCAGGCGCTTCTGtgcaCTGGTGGAGAAG
Tir_{EPEC} fwd	GAGA**GGATCC**GTTGAAAGCAATGCACAGGCGC
Tir_{EPEC} rev	GAGA**GAATTC**TTAAACGAAACGTACTGGTCCC
Tir_{EHEC} fwd	GAGA**AGATCT**ATTGAAAATAATGCTCAGGCG
Tir_{EHEC} rev	GAGA**GAATTC**TTAGACGAAACGATGGGATCCC

Table S2: constructs used in this study

construct	**entry**	**Residues** (AA)	**vectors**
I-BAR $_{IRSp53}$ wt	NM_017450	**1-250**	pQTEV, pEGFP-C1
I-BAR $_{IRSp53}$ L28E	derivative of above	as above	pQTEV, pEGFP-C1
I-BAR $_{IRSp53}$ K108A	derivative of above	as above	pQTEV, pEGFP-C1
I-BAR $_{IRSp53}$ R193S	derivative of above	as above	pQTEV, pEGFP-C1
I-BAR $_{IRSp53}$ F196A	derivative of above	as above	pQTEV, pEGFP-C1
I-BAR $_{IRSp53}$ K108A/R193S	derivative of above	as above	pQTEV, pEGFP-C1
I-BAR $_{IRSp53}$ K108A/F196A	derivative of above	as above	pQTEV, pEGFP-C1
Tir_{EPEC} C-terminus	NC_011601 (4113830-4115482)	337-551	pEGFP-C1
Tir_{EHEC} C-terminus	NC_002655 (4668913-4670589)	334-558	pEGFP-C1
Tir_{EHEC} C-terminus	NC_002655	385-558	pAG416GAL-μNS-ccdB
Tir_{EHEC} C-terminus	NPY->AAA	385-558	pAG416GAL-μNS-ccdB
I-BAR $_{IRTKS}$ wt	NM_018842.4	as above	pAG415GAL-GFP-ccdB
I-BAR $_{IRTKS}$ L27E	derivative of above	as above	pAG415GAL-GFP-ccdB
I-BAR $_{IRTKS}$ K107A	derivative of above	as above	pAG415GAL-GFP-ccdB
I-BAR $_{IRTKS}$ R192S	derivative of above	as above	pAG415GAL-GFP-ccdB
I-BAR $_{IRTKS}$ F195A	derivative of above	as above	pAG415GAL-GFP-ccdB
I-BAR $_{IRTKS}$ K107A/R192S	derivative of above	as above	pAG415GAL-GFP-ccdB
I-BAR $_{IRTKS}$ K107A/F195A	derivative of above	as above	pAG415GAL-GFP-ccdB

Table S3, related to Figure 6: Potential NPY-containing interactors of I-BAR proteins

Short name	Full name	HGNR	NPY position	NPY location	Protein class
PK3CB	Pi3K, p110b, Phosphtidylinositol-3 kinase, catalytic subunit	8976	482-84	C2 domain	phospholipid kinase
ROCK2	Rho-associated protein kinase 2	10252	1195-97	very C-terminus	protein kinases
LIMK1 & -2	LIM domain kinase 1	6613	512-14	kinase domain	
ITSN1 & -2	Intersectin 1 (Cdc42 GEF)	6183	1618-20	C2 domain	regulators of Rho-GTPase activity
ARHGAP10	GRAF2 GAP10 associated with FAK (RhoA, Cdc42)	26099	625-27	between Rho-GAP and SH3	
Myo IA	Brush border myosin 1 /BBM-I	7595	49-51	head domain	myosins
Myo X	Myosin 10 (filopodia)	7593	104-06	head domain	
MyoXV	Myosin 15 (stereocilia)	7594	423-25 1263-65	head domain NT head domain CT	
CLAP1 & -2	CLIP115 associated protein1	17088	1265-67	CLIP-binding site	microtubule tip proteins
SHANK2	SH3 and multiple ankyrin repeat domains protein 2	14295	608-10	central part	partners of IRSp53
BAI2	Brain-specific inhibitor of angiogenesis 2 (GPCR)	944	1417-19	cytoplasmic tail	

The SwissProt database comprises 20,329 human proteins, of which 749 contain the NPY motif as detected using Scansite (http://scansite.mit.edu/dbsequence_one.html). Candidates that potentially might interact with I-BAR domains of IRSp53 or IRTKS were selected according to the following criteria: (i) nuclear, intraluminal or extracellular motifs are excluded; (ii) the motif is conserved at least between human and mouse orthologs and (iii) conservation between paralogs is preferred. The selection shown in Table S1 was further confined based on involvement in IRSp53-signalling (e.g. Shank), in cytoskeleton reorganisation (e.g. LIMK), in Rho-GTPase signalling (Intersectin), and for those that were implicated in filopodium (or similar like stereocilia/microvilli, e.g. Myosin X) formation before.

Supplemental Experimental Procedures

Plasmids

A PCR fragment encoding amino acids 1-250 (MSLS…VASN) of human IRSp53 (SwissProt BAIP2_HUMAN) was obtained from a GST-IRSp53-I-BAR clone (Weiss et al., 2009) and cloned with BamHI and NotI into pQTEV (GenBank AY243506), resulting in I-BAR$_{IRSp53}$ fused to an N-terminal His$_7$-tag and TEV cleavage site with the sequence GSTMSLS…VASN upon cleavage. Mutations were introduced by site directed mutagenesis (QuikChange kit, Stratagene). All primers are listed in the Table S1 and S2. Wild type and mutant I-BARs of IRSp53 were subcloned to pEGFP-C1 (Clontech) using BglII and Bsp120I. TirC of EHEC O157:H7 strain EDL933 (aa 337-558) (Griffin et al., 1988) and EPEC O127:H6 strain E2348/69 (aa 334-550) (Levine et al., 1978) were described (Weiss et al., 2009). For PIP assays (Schmitz et al., 2009), EHEC TirC (aa 385-558) the corresponding TirC NPY$_{458}$→AAA$_{458}$ mutant, and the I-BAR domain of human IRTKS (SwissProt BI2L1_HUMAN, aa 1-250) were amplified by PCR using primers flanked by attB recombination sites and were introduced in pDONR221 to create Gateway entry vectors (Invitrogen) *via* BP reactions. Inserts were sequenced and transferred *via* LR reactions (Invitrogen) into Gateway destination vectors pAG416GAL-μNS-ccdB (Schmitz et al., 2009) and pAG415GAL-GFP-ccdB (Alberti et al., 2007) to create μNS-TirC, μNS-TirC AAA$_{458}$ and GFP-I-BAR$_{IRTKS}$ fusions,

respectively. Mutations were generated in I-BAR$_{IRTKS}$ by inverse PCR following the SLIM methodology (Chiu et al., 2004) and using the entry clone pDONR221-I-BAR$_{IRTKS}$ as template. After sequencing, I-BAR domain mutant genes were transferred in plasmid pAG415GAL-GFP-ccdB *via* LR reactions.

Supplemental References

Alberti, S., Gitler, A.D., and Lindquist, S. (2007). A suite of Gateway cloning vectors for high-throughput genetic analysis in Saccharomyces cerevisiae. Yeast *24*, 913-919.

Chiu, J., March, P.E., Lee, R., and Tillett, D. (2004). Site-directed, Ligase-Independent Mutagenesis (SLIM): a single-tube methodology approaching 100% efficiency in 4 h. Nucl Acids Res *32*, e174-.

Griffin, P.M., Ostroff, S.M., Tauxe, R.V., Greene, K.D., Wells, J.G., Lewis, J.H., and Blake, P.A. (1988). Illnesses associated with Escherichia coli O157:H7 infections. A broad clinical spectrum. Annals of internal medicine *109*, 705-712.

Levine, M.M., Bergquist, E.J., Nalin, D.R., Waterman, D.H., Hornick, R.B., Young, C.R., and Sotman, S. (1978). Escherichia coli strains that cause diarrhoea but do not produce heat-labile or heat-stable enterotoxins and are non-invasive. Lancet *1*, 1119-1122.

Millard, T.H., Bompard, G., Heung, M.Y., Dafforn, T.R., Scott, D.J., Machesky, L.M., and Fütterer, K. (2005). Structural basis of filopodia formation induced by the IRSp53/MIM homology domain of human IRSp53. Embo J *24*, 240-250.

Schmitz, A.M., Morrison, M.F., Agunwamba, A.O., Nibert, M.L., and Lesser, C.F. (2009). Protein interaction platforms: visualization of interacting proteins in yeast. Nat Meth *6*, 500-502.

Weiss, S.M., Ladwein, M., Schmidt, D., Ehinger, J., Lommel, S., Städing, K., Beutling, U., Disanza, A., Frank, R., Jänsch, L.*, et al.* (2009). IRSp53 links the enterohemorrhagic E. coli effectors Tir and EspF$_U$ for actin pedestal formation. Cell Host Microbe *5*, 244-258.